

BRIGHAM YOUNG UNIVERSITY

GEOLOGY STUDIES

VOLUME 27, PART 1

AUGUST 1980

BRIGHAM YOUNG UNIVERSITY GEOLOGY STUDIES

Volume 27, Part 1

Preble Formation, a Cambrian Outer Continental Shelf Deposit in Nevada	M. N. Rees and A. J. Rowell
The Fitchville Formation: A Study of the Biostratigraphy and Depositional Environments in West Central Utah County, Utah	Brian R. Greenhalgh
Sandstone and Conglomerate-Breccia Pipes and Dikes of the Kodachrome Basin Area, Kane County, Utah	Cheryl Hannum
Exhumed Paleochannels in the Lower Cretaceous Cedar Mountain Formation near Green River, Utah	Daniel R. Harris
The Stratigraphy and Structure of the Cedar Hills, Sanpete County, Utah	Ralph L. Hawks, Jr.
Paleoenvironments of the Lower Triassic Thaynes Formation, near Diamond Fork in Spanish Fork Canyon, Utah County, Utah	Bruce H. James
A Gravity Study of the Nampa-Caldwell Area, Canyon County, Idaho	J. Roger Olsen
Geology of the Sterling Quadrangle, Sanpete County, Utah	James Michael Taylor

Publications and Maps of the Geology Department



Cover: Aerial photograph showing exhumed stream paleochannels in the Cedar Mountain Formation near Green River, Utah. Courtesy Daniel R. Harris.

A publication of the
Department of Geology
Brigham Young University
Provo, Utah 84602

Editors

W. Kenneth Hamblin
Cynthia M. Gardner

Brigham Young University Geology Studies is published by the department. *Geology Studies* consists of graduate-student and staff research in the department and occasional papers from other contributors. *Studies for Students* supplements the regular issues and is intended as a series of short papers of general interest which may serve as guides to the geology of Utah for beginning students and laymen.

ISSN 0068-1016
Distributed August 1980
8-80 600 43937

CONTENTS

Preble Formation, a Cambrian Outer Continental Shelf Deposit in Nevada	1	Biostratigraphy	23
Abstract	1	The lower (Famennian) limestones (units 2a and 2b)	23
Introduction	1	The lower (Famennian) dolomites (units 3-5)	24
Preble Formation	1	The upper (Kinderhookian) dolomites (units 6 and 7)	24
Definition and age	1	The upper (Kinderhookian) limestones (units 8-10)	25
Thickness and stratigraphic subdivision	2	The lowermost (Osagean) Gardison limestones (units 11-14)	25
Interpretation of lithology and depositional setting	3	Conclusions	25
Lower Preble Formation	3	Appendix A	25
Middle Preble Formation	4	Appendix B	27
Upper Preble Formation	7	References cited	29
Acknowledgments	8	Figures	
References cited	8	1. Index map of the study area	10
Figures		2. Wanlass Hill viewed from the south	10
1. Principal outcrops of Preble Formation and index of localities mentioned in text	1	3. Greeley Hill viewed from the southwest	11
2. Outcrop patterns of gravity-flow deposits and principal faults	2	4. Basal sand-grain layer (unit 1)	12
3. Geological sketch map	3	5. Stratigraphy, correlation, and zonation chart	13
4. Thrust recumbent folds	3	6. Association of <i>Syringopora surcularia</i> and <i>S. hisingeri</i> ...	16
5. Negative print of bioclastic grainstone	4	7. Carbonate sedimentation model of Irwin (1965)	17
6. Outcrop of alternating carbonate turbidity deposits and shale	5	8. Photomicrograph of basal sand-grain layer	17
7. Sediment gravity-flow deposit	5	9. Sand-filled burrows of unit 5	18
8. Oolite with interbeds and lenses of dolomitic mudstone	6	10. Distorted <i>Syringopora</i> and burrowed layer of unit 5 ...	18
9. Photomicrograph: Contact between oolite and overlying dolomitic mudstone	6	11. Photomicrograph of intraclasts in unit 9	20
10. Upper Cambrian thin-bedded dolomitic limestone and shale	6	12. Curly bed, with stromatolitic dome	21
		13. Photomicrograph of the curly-bed laminations	22
		14. Photomicrograph of the curly bed with <i>Sphaerocodium</i> ?	22
		Tables	
		1. Abundances of <i>Syringopora</i> corals on Wanlass Hill	11
		2. Abundances of solitary rugose corals on Wanlass Hill	11
The Fitchville Formation: A Study of the Biostratigraphy and Depositional Environments in West Central Utah County, Utah	9	Sandstone and Conglomerate-Breccia Pipes and Dikes of the Kodachrome Basin Area, Kane County, Utah	31
Introduction	9	Abstract	31
Acknowledgments	9	Introduction	31
Previous work	9	Location	31
Procedures	10	Previous work	31
Paleogeography and paleotectonic setting	11	Methods of study	32
Stratigraphy	12	Structure and regional setting	33
Stratigraphic units	12	Acknowledgments	34
Dolomitization	14	Stratigraphy	34
Paleoecology	14	Navajo Sandstone	34
The paleoecology of Fitchville corals	14	Carmel Formation	34
The paleoecology of Fitchville brachiopods	14	Judd Hollow Tongue	34
The paleoecology of conodonts	15	Thousand Pockets Tongue of the Navajo Sandstone	34
Orientations	15	Paria River Member	34
Associations	15	Winsor Member	34
Abundances	15	Wiggler Wash Member	34
Depositional environments	17	Entrada Sandstone	35
Introduction	17	Gunsight Butte Member	35
Quartz clastic layers	17	Cannonville Member	35
The lower (Devonian) limestones (units 2a and 2b) ..	19	Escalante Member	35
The lower (Devonian) dolomites (units 3-5)	19	Pre-Morrison unconformity	36
The upper (Mississippian) dolomites (units 6 and 7) ..	20	Henrieville Sandstone	36
The upper (Mississippian) limestones (units 8 and 9) ..	20	Sub-Cretaceous unconformity	36
The curly limestone (unit 10)	20	Dakota Formation	36
The lowermost Gardison limestones (units 11-14) ..	23		

Distribution of pipes and dikes	36	30. Photomicrograph: Thin section of thin dike between pipes 10 and 11	47
Description of representative pipes and dikes	36	Exhumed Paleochannels in the Lower Cretaceous Cedar Mountain Formation near Green River, Utah	51
Pipe 3	36	Abstract	51
Pipe 27	36	Introduction	51
Pipe 28	37	Location	51
Pipe area 29	37	Previous work	51
Pipe 34	39	Methods	53
Pipe 35	39	Acknowledgments	53
Pipe 38	40	Geologic setting	53
Pipe 43	40	Stratigraphy	53
Dike 49	40	Morrison Formation	54
Pipe 51	41	Cedar Mountain Formation	54
Pipe 52	41	Dakota Formation	54
Composition	41	Mancos Formation	54
Country rock	41	Channel classification	56
Sandstone and conglomerate pipes and dikes	43	Channel dimensions	56
Generalized types of pipes and dikes in the Kodachrome Basin area	45	Channel A	56
Sandstone pipes	45	Channel B	56
Conglomerate-breccia pipes	45	Channel C	56
Thick extensive dikes	46	Channel D	57
Thin dikes	46	Channel patterns	57
Conclusions	46	Sinuosity	58
Observations and comparisons	46	Point-bar and channel-fill deposits	58
Interpretation	48	Point-bar deposits	58
References cited	49	Channel fills	60
Figures		Sedimentary structures	60
1. Index map	31	Primary structures	60
2. Stratigraphic section	32	Secondary structures	61
3. Stratigraphy from Gunsight Butte Member of Entrada Sandstone to Dakota Formation	33	Vertical sequence	62
4. Physiographic map of southwestern Colorado Plateau	34	Paleochannel characteristics	63
5. Map pipe location and stratigraphy, with joint roses	35	Current direction	64
6. Map outline of pipe 3	36	Composition and source area	64
7. Map outline of pipe area 29	37	Conclusion	65
8. Map outline of pipe 35	38	References cited	65
9. Map outline of pipe 43	38	Figures	
10. Map outline of pipe 51	38	1. Index map	51
11. Map outline of pipe 52	38	2. Aerial photograph of western thesis area	52
12. Photograph of pipe 3	39	3. Stratigraphic column	53
13. Photograph of sandstone block of pipe 5	39	4. Geologic map	55
14. Photograph of interior of pipe 3	39	5. Bifurcation of channel B (photo)	57
15. Photograph of fracture at pipe edge of pipe 26	40	6. Map of channel A, segment 2	58
16. Photograph of pipe complex 29	41	7. Map of channel B, segments 5, 6, 7, and 8	59
17. Photograph of thin dike complex of pipe 29	42	8. Map of channel D, segment 6	59
18. Photograph of main "feeder" dikes and extensions of thin dike complex pipe area 29	42	9. Map of channel C, segments 2 and 3	60
19. Photograph of pebbly interior of lowermost thin dikes of pipe complex 29	42	10. Accretion ridge	61
20. Photograph of pipe 35	42	11. Erosional surface channel fill	61
21. Photomicrograph of gradational edge of pipe 35	43	12. Erosional surface channel fill	61
22. Photograph of base of pipe 35	43	13. Trough cross-beds	62
23. Photograph of northern face of pipe 43	43	14. Planar cross-beds	62
24. Photograph of sandstone and mudstone blocks at base of pipe 43	44	15. Climbing ripples	62
25. Photomicrograph: Thin section of interior of pipe 47	44	16. Scour-and-fill deposits	62
26. Photograph of pipe 52	44	17. Graded bedding in trough cross-beds	63
27. Histogram of grain-size distribution	45	18. Chert-cemented structure	63
28. Photomicrograph: Thin section of pebbly interior of pipe 3	46	19. Grading at base of channel A	63
29. Photograph of converging dikes between pipes 10 and 11	47	20. Vertical sequence of channel A	64
		21. Cross section of a point bar in channel D	65
		Tables	
		1. Paleochannel characteristics	64
		2. Channel composition	65

The Stratigraphy and Structure of the Cedar Hills, Sanpete County, Utah	67
Abstract	67
Introduction	67
Previous work	67
Acknowledgments	67
Geologic setting	68
Eocambrian to Jurassic	68
Jurassic to Cretaceous	68
Cretaceous to Eocene	68
Oligocene	68
Miocene to Recent	68
Present-day setting	68
Stratigraphy	69
Cretaceous-Tertiary	70
North Horn Formation	70
Tertiary	70
Flagstaff Formation	70
Colton Formation	72
Green River Formation	72
Tertiary volcanic rocks	73
Tertiary-Quaternary	74
Stream gravels	74
Landslides	74
Quaternary	75
Alluvium	75
Structure	75
Tectonic history	77
Economic geology	77
Summary	79
References cited	79

Figures

1. Index map	67
2. Stratigraphic column of rocks exposed in study area	69
3. Bedrock geology map	70
4. North Horn Formation	71
5. Outcrop of North Horn Formation	71
6. Outcrop of Flagstaff Formation	71
7. Colton Formation	72
8. Green River Formation	73
9. Large landslide in Big Hollow involving Colton and Green River Formations	74
10. Rounded cobbles of water-laid conglomerate	75
11. Landslide involving Tertiary volcanic rocks	75
12. Large quartzite boulder	76
13. Steplike terraces in stream gravels	76
14. View of Big Hollow	76
15. Aerial view of Water Hollow	76
16. Recent landslide in Big Hollow involving Green River Formation	77
17. Geologic map of study area and cross section in pocket	
18. Orogenic evolution of study area	78

Paleoenvironments of the Lower Triassic Thaynes Formation, near Diamond Fork in Spanish Fork Canyon, Utah County, Utah

Abstract	81
Introduction	81
Location	81
Geologic setting and stratigraphy	82
Previous work	83
Methods	84
Acknowledgments	84

Lithology	84
Sandstone	84
Red to purple sandstone	85
Orange to brown sandstone	85
Olive gray to greenish gray sandstone	85
Yellow to grayish yellow sandstone	85
Very pale yellowish green to light greenish gray sandstone	85
Siltstone	88
Brownish red to pale red and pale red purple siltstone	88
Olive to greenish gray and grayish yellow green siltstone	88
Yellow, brown, and grayish orange siltstone	89
Shale	89
Claystone and mudstone	89
Limestone	89
Mudstone	89
Wackestone	89
Packstone	90
Grainstone	90
Floatstone	90
Bindstone	90
Cyclic patterns	91
Sedimentary structures	92
Cross-bedding	93
Flaser bedding	93
Lenticular bedding	93
Paleontology	93
Occurrence and preservation	93
Body fossils	93
Crinoids	94
Echinoids	94
Conodonts	94
Foraminifera	94
Brachiopods	94
Fish fragments	95
Sponges	95
Ostracodes	95
Steinkerns	95
Bivalves	95
Gastropods	95
Algal stromatolites	96
Ichnofossils	96
Paleoenvironment	96
Paleoclimate	96
Currents and energy levels	96
Sedimentary model	96
Marine	96
Subtidal	97
Intertidal	98
Supratidal	98
Summary	98
References cited	99

Figures

1. Index map of study area	81
2. Stratigraphic column	82
3. Conodont zonation and age assignment of rocks of study area	83
4. Detailed stratigraphic section of study area	86, 87
5. Low cross-bed sets	88
6. Double-trail pascichnia	88
7. Photomicrograph: Sponge spiculite	89
8. Domichnia and vertical burrows	90

9. Mud clast with bivalve and ostracode valves	90	11. Gravity profile b-b' and 2 1/2-dimensional interpretive model	112
10. Crinoid ossicles with algal and fecal pellets	90	12. Gravity profile c-c' and 2 1/2-dimensional interpretive model	112
11. Photomicrograph: Grainstone	91	13. Gravity profile d-d' and 2 1/2-dimensional interpretive model	112
12. Photomicrograph: Algal stromatolite	91	14. Gravity profile e-e'	113
13. Generalized representation of 3- and 5-element cycles of measured section	91	15. Gravity profile f-f' and 2 1/2-dimensional interpretive model	113
14. Typical 5-element cycle in units 169 to 174	92	16. Gravity profile g-g' and 2 1/2-dimensional interpretive model	113
15. Symmetrical current ripples in coarse siltstone	92	17. Gravity profile g-g' and 2 1/2-dimensional interpretive model (alternative interpretation)	114
16. Undulatory to lingoid current ripples in red siltstone	92	18. Gravity profile g-g' and 2 1/2-dimensional interpretive model (alternative interpretation)	114
17. Micro-cross-lamination in red siltstone of unit 89	93		
18. Lyssakid hexactinellid sponges	95		
19. Energy index of rocks of measured section	97		
20. Transgressive-regressive sequences in the Thaynes Formation	99		
A Gravity Study of the Nampa-Caldwell Area, Canyon County, Idaho			
Abstract	101	Geology of the Sterling Quadrangle, Sanpete County, Utah	117
Acknowledgments	101	Abstract	117
Introduction	101	Introduction	117
Previous work	101	Location	117
Current work	101	Previous work	117
Regional geologic setting	101	Stratigraphy	117
Structural geology of the Nampa-Caldwell area	102	Jurassic System	118
Stratigraphy	104	Arapien Shale	118
Data acquisition and reduction	104	Cretaceous System	118
Instrumentation	104	Sanpete Formation	118
Survey technique	104	Allen Valley Shale	118
Data reduction	104	Funk Valley Formation	120
Terrain corrections	105	Sixmile Canyon Formation	120
Reliability of data	105	Price River Formation	120
Gravity data analysis	105	Cretaceous-Tertiary	120
Terrain-corrected Bouguer gravity anomaly map	105	North Horn Formation	120
Third-order residual gravity anomaly map	107	Tertiary	120
Regional gravity map	107	North Horn Formation	120
Interpretation	107	Tertiary System	121
Residual gravity anomaly map—General remarks	107	Flagstaff Formation	121
Profile modeling	111	Colton Formation	121
Gravity profile a-a' and interpretive model	111	Green River Formation	121
Gravity profile b-b' and interpretive model	111	Crazy Hollow Formation	122
Gravity profile c-c' and interpretive model	112	Quaternary System	122
Gravity profile d-d' and interpretive model	112	Structural geology	123
Gravity profile e-e'	113	East region	123
Gravity profile f-f' and interpretive model	113	Faults	123
Gravity profile g-g' and interpretive model	113	Diapir	123
Summary and conclusions	114	Unconformities	123
References cited	114	Central region	124
		Diapir	124
		Unconformities	125
Figures		West region	126
1. Index map	101	Faults	126
2. Topographic map	102	Diapir	126
3. Preliminary geologic map of the Nampa-Caldwell area	103	Unconformities	127
4. Stratigraphic column	104	Geologic history	127
5. Terrain-corrected Bouguer gravity anomaly map	106	Jurassic Period	127
6. Instrument-performance record for time data	107	Cretaceous Period	127
7. Third-order polynomial model	108	Tertiary Period	129
8. Third-order polynomial residual gravity anomaly map	109	Economic geology	129
9. Third-order polynomial residual gravity anomaly map	110	Conclusions	129
10. Gravity profile a-a' and 2 1/2-dimensional interpretive model	111	Acknowledgments	130
		Appendix	130
		References	135

Figures	
1. Index map	117
2. Aerial view of Sterling Quadrangle	118
3. Stratigraphic column	119
4. Geologic map and cross sections	in pocket
5. Photomicrograph: Charophytes and gastropod fragments in freshwater limestone	121
6. Photomicrograph: Oncolite	121
7. Photomicrograph: Brecciated limestone	122
8. Oncolite conglomerate facies	122
9. Photomicrograph: Clasts in Quaternary gravels	123
10. Locations and elevations of Quaternary gravels	123
11. Large landslide in Forbush Cove	124
12. Landslide in Green River Formation	124
13. Three regions in Sterling Quadrangle	124
14. West flank of Wasatch Monocline and east flank of anticline	125
15. Double angular unconformity at mouth of Sixmile Canyon	125
16. Angular unconformity at south end of San Pitch Mountains	125
17. Unconformity: Green River Formation on Arapien Shale	126
18. Unconformity: Quaternary gravels on overturned Arapien Shale	126
19. North Horn Formation beds overturned	127
20. Upright beds caught in lower units folded over by diapir	127
21. Syncline in North Horn Formation	127
22. Comparison of structural configuration proposed in this study and that proposed by Gilliland (1963)	128
23. Schematic representation of structural development of Sterling Quadrangle	130, 131
Publications and maps of the Geology Department ... 137	

A Gravity Study of the Nampa-Caldwell Area, Canyon County, Idaho*

J. ROGER OLSEN

Texaco
P.O. Box 52332
Houston, Texas 77052

ABSTRACT.—A gravity study of the Nampa-Caldwell area is part of an integrated geological and geophysical study being done by the Idaho Department of Water Resources, Geothermal Division, for the purpose of evaluating the geothermal potential of the area. Gravity was measured at 680 stations with a Worden Geodest Gravimeter in an area of 182 square miles. A terrain-corrected Bouguer anomaly map was produced which shows: (1) a strong (15–20 mgal) northwest trending gravity high; (2) linear anomalies trending north-south and east-west; and (3) high spatial frequency anomalies with complex orientation. The northwest-trending gravity high is a regional anomaly probably caused by a thick accumulation of volcanic material in a fault-bounded or downwarped structural trough. A third-order polynomial residual map was chosen to emphasize local, near-surface anomalies and depress the regional anomaly. The residual linear-trending anomalies were interpreted as buried faults, but they could result from a buried low-density erosional remnant. A residual gravity high (3 mgals) centered near Lake Lowell was interpreted as a possible near-surface basalt flow, but it may also be an artifact of map processing. The high-frequency anomalies probably represent structural complexities in near-surface basalt flows. Two and one-half dimensional modeling (i.e., finite strike length and constant polygonal cross section) shows general magnitudes and possible configurations of anomaly-producing bodies, but it is not possible to deduce specific geologic structures from gravity data alone.

ACKNOWLEDGMENTS

I wish to thank Dr. John R. Pelton, who served as committee chairman and gave invaluable assistance throughout this project. Also, I would like to thank Dr. Myron G. Best, who served as a committee member, and Dr. Spencer H. Wood, who provided geologic control information and consultation. My thanks are extended to Ralph Melon and John Mitchell and others of the Idaho Department of Water Resources for their assistance during various phases of this study. I am grateful to my wife, Sandra, who served as my field assistant and aided in typing and data handling, and to my parents, Mr. and Mrs. John Olsen, for their support.

INTRODUCTION

A gravity study of the Nampa-Caldwell area in Canyon County (figs. 1, 2) is part of an integrated geological and geophysical program being conducted by the Idaho Department of Water Resources, Geothermal Division. The overall objective of the program is to evaluate the geothermal potential of the Nampa-Caldwell area. The purpose of the gravity study is twofold: (1) compile a terrain-corrected Bouguer gravity anomaly map and a residual gravity anomaly map, and (2) produce interpretive models of gravity profiles in areas where well-defined anomalies exist.

Previous Work

The geology and mineral resources of Ada and Canyon Counties is summarized by Savage (1958). Malde and others (1962) review upper Cenozoic stratigraphy, and Newton and Corcoran (1963) present stratigraphic information from wells within or near the study area that aids in stratigraphic correlation and interpretation of subsurface geologic structures. Mabey and others (1974) compiled a preliminary gravity map

of southern Idaho, and Mabey (1976) published an interpretation of this map, including two-dimensional interpretive models. Several deep exploration wells have been drilled in or near the study area, logs of which are available from the Idaho Bureau of Mines and Geology.

Current Work

In addition to the gravity study of the Nampa-Caldwell area, several other concurrent geologic investigations are being conducted under the direction of the Idaho Department of Water Resources, Geothermal Division. These include correlation of water well data (Anderson unpublished preliminary study 1979); geochemical investigation (Mitchell pers. comm. 1979); photolineament study (Anderson unpublished 1979); heat flow study (Mitchell pers. comm. 1979); and detailed geologic mapping (Wood preliminary map and report in preparation 1979).

Regional Geologic Setting

The Nampa-Caldwell area is located in the Malheur-Boise Basin section of the High Lava Plains subprovinces of the Columbia Intermontane geomorphic province (Freeman and others 1945). This section forms a deep northwest-trending struc-

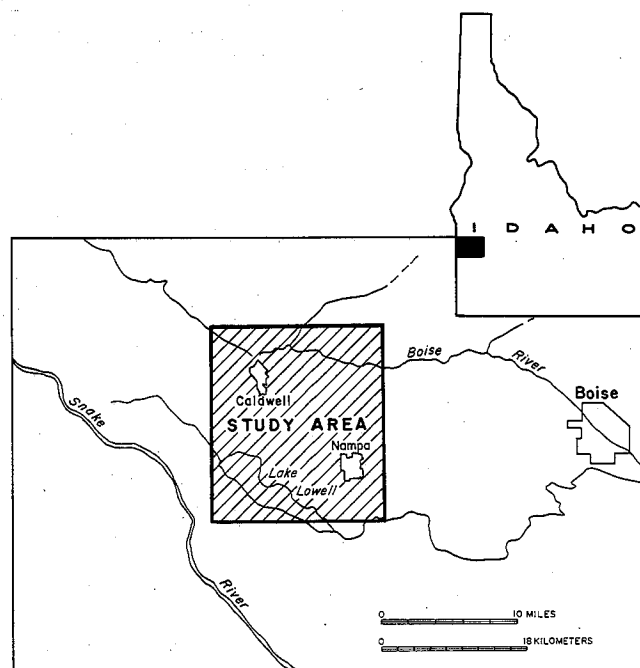


FIGURE 1.—Index map showing location of study area.

*A thesis presented to the Department of Geology, Brigham Young University, in partial fulfillment of the requirements for the degree Master of Science, August 1979. Thesis chairman: John R. Pelton.

tural trough, the upper part of which is filled with a thick sequence of clastic sediments of streams, playas, and lakes, interlayered with volcanics. Relief is low, and there is an almost complete cover of sediment and basaltic flows.

Gravity data and, to a lesser extent, aeromagnetic data indicate that basaltic infill of the lower part of the trough is from 2½ miles to as much as 7 miles thick (Mabey 1976). The amount of interlayered sediment in the lower trough is unknown. These basalts have been displaced downward by pro-

gressive crustal thinning due to rifting throughout most of the Cenozoic (Warner 1977). The Idaho batholith presumably underlies the entire study area at an unknown depth (Taubeneck 1971).

Structural Geology of the Nampa-Caldwell Area

The area is situated in a structural zone having a strong northwest trend as indicated by regional gravity, regional aeromagnetics, photolineaments, and surface mapping. A north-

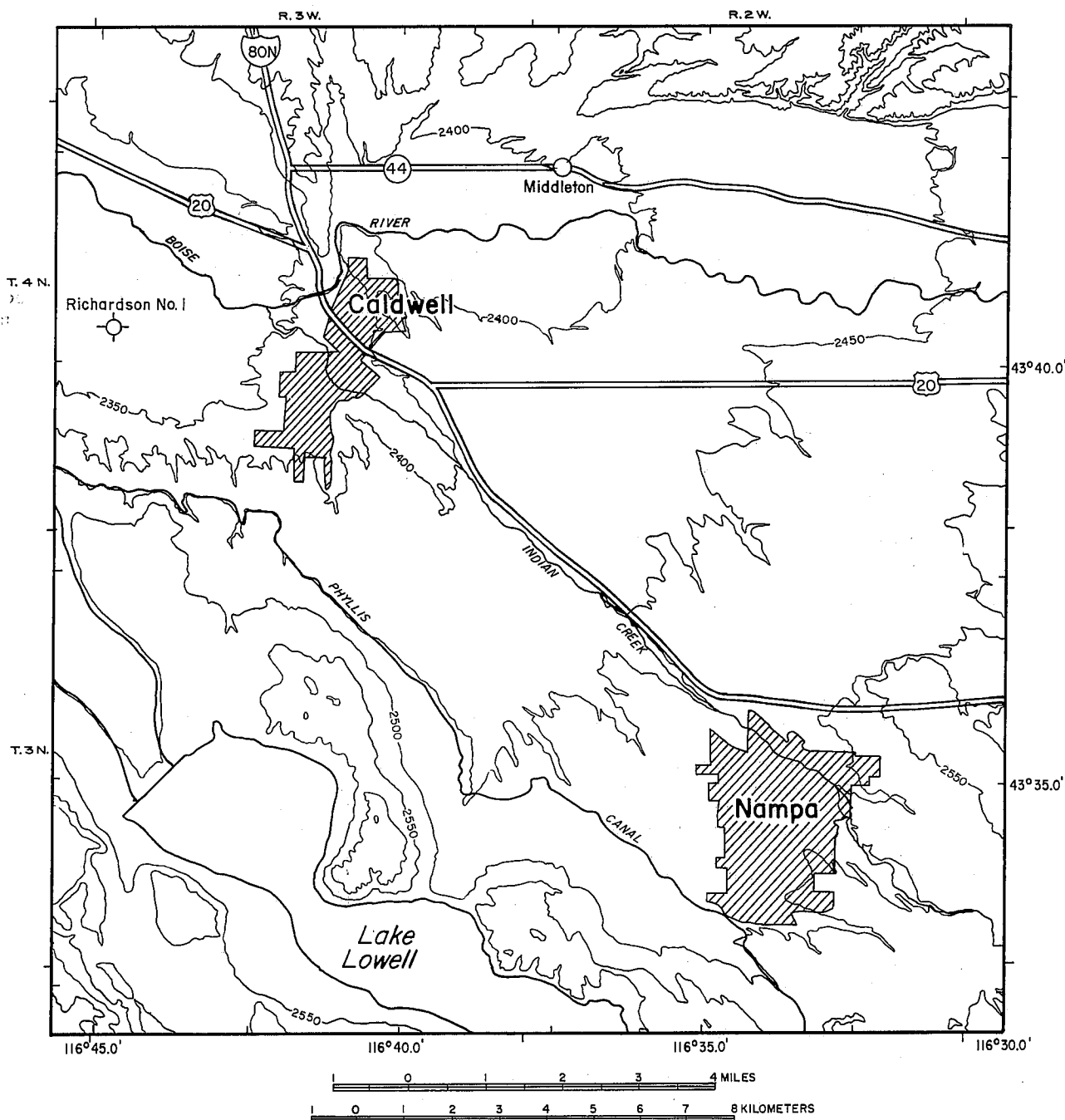
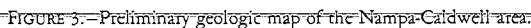


FIGURE 2.—Topographic map of study area showing location of Nampa and Caldwell as well as major roads, drainage features, Lake Lowell, and Richardson No. 1 well.

Surface mapping indicates a region at least 6 miles wide of normal faulting in the Lake Lowell area (fig. 3). The fault zone may extend farther northward, but there is no topographic expression to indicate that it does. All faults strike north-



westward, and dips are measured from 50° to 85°. Offsets range to more than 100 feet in some cases, as indicated in driller's logs (John Anderson pers. comm. 1979). The faults were probably active from 1.1 to 1.7 million years ago (Birkeland and others 1971). This activity was probably contemporaneous with basaltic eruptions (Wood pers. comm. 1979).

Correlation of deep exploration well logs in or near the study area is currently under way. Preliminary findings of this correlation show a structural basalt high north and northwest of Nampa. Drill-hole correlation also indicates a great deal of structural complexity in the subsurface Miocene units (Wood pers. comm. 1979).

Stratigraphy

An understanding of stratigraphy is essential to the interpretation of gravity data. From stratigraphic information inferences may be made as to subsurface densities and depths of given stratigraphic horizons. A detailed stratigraphic column is shown in figure 4 based on data and interpretations of Spencer H. Wood and is used here with his permission. It is based on correlation of logs of five deep wells in or near the study area and on surface mapping.

DATA ACQUISITION AND REDUCTION

Instrumentation

All gravity readings for this survey were taken with a Worden Geodetic Gravimeter No. 735 which has a precision capability of 0.01 mgal. The scale constant for this instrument is 0.1247(3) mgals per dial division. Elevation for two detailed gravity profiles were determined using a Keuffel and Esser Carl Ziess self-leveling level.

Survey Technique

Gravity stations were located on published 7½-minute United States Geological Survey topographic quadrangle maps. Where practical the stations were placed on a 0.5-mile grid on section corners and quarter corners. Vertical control was obtained from bench marks, corner elevations, or spot elevations or was interpolated directly from topographic contours. A hand level was used to adjust elevations to stations when necessary.

For two detailed gravity profiles, stations were chained on a 500-foot interval, and the levels were read to the nearest 0.1 foot. The level lines were not closed because of the short profile lengths and relative flatness of the topography. On a third detailed gravity profile along Interstate 80, elevations were obtained from interstate highway plans. The purpose of the detailed profiles is to provide more precise gravity values on which to base 2½-dimensional models.

All gravity stations were tied to a common base station (station no. 1) at a second-order Bureau of Reclamation bench mark (located near the southeast corner of "Gabe's Auto Parts") in Caldwell. Station no. 1 was occupied at least twice a day. Intermediate field base stations were established and tied to station no. 1 by a series of loops and occupied every three to four hours to correct for drift. The sequence of stations for a day's work was ABCDEBFGHBA, A being station no. 1, B being a field base, and the rest being gravity stations. The stations were numbered consecutively from 1 to 680. The gravimeter was read twice at each station, and, where the difference exceeded 0.3 dial divisions (about 0.04 mgals), it was read again until two consecutive readings fell within that tolerance.

At each station the following information was recorded: station number, elevation to the nearest foot, time to the near-

est five minutes, instrument temperature to the nearest degree Fahrenheit, at least two gravimeter readings, and remarks such as location, interference, elevation reliability, etc. The station locations were also marked on maps using a numbered pinprick on the back of 7½-minute topographic quadrangle sheets. The field techniques are based on those recommended by Dobrin (1976, p. 404-10) and Telford and others (1978, p. 43-48).

Data Reduction

Reduction of gravimeter readings to simple Bouguer gravity anomaly values was accomplished using a gravity reduction program developed at the University of Utah. The program was adapted for use on the IBM System 360 at Brigham Young University, where the reduction was done.

The reduction program converts gravimeter readings to observed gravity values according to the following equation:

$$g(S) = g(B) + (R_s - R_B) (0.12473) \quad (1)$$

DEPTH (FEET)	AGE	GROUPS & FORMATIONS	LITHOLOGY	DESCRIPTION	DEPTH (MET.)
1000	PLEISTOCENE	Snake River Group		TERRACE GRAVELS OF THE BOISE RIVER DRAINAGE	
		Glenns Ferry Formation		DASALT, DARK GRAY, TITANIO-MAGNETITE, PLAGIOCLASE, AND OLIVINE - 2 FLOWS, 3 TO 15 M THICK, CONFINED TO INDIVIDUAL CREEKS AND LAKE BASINS	
				SILT, SAND, LIGHT BROWN, FINE GRAINED, POORLY SORTED	
				CLAYSTONE, MEDIUM BROWN TO LIGHT GRAY (BLUE CLAY IN WATER-WELL DRILLER'S LOGS)	
				SILT, SAND, AND CLAYSTONE, LIGHT BROWN TO LIGHT GRAY, ELECTRIC LOGS INDICATE SANDS ARE FAIR ROUTERS	
2000	PLIO- PLEISTOCENE	Chalk Hills Formation (?)		SAND, GRAY, VERY FINE TO MEDIUM GRAINED, FAIR SORTING, ELECTRIC LOGS INDICATE GOOD AQUIFER	500
				SILTSTONE, GRAY-GREEN	
3000				BASALT, DARK GRAY TO BLACK, ABUNDANT OLIVINE	
		Grassy Mountain Formation		TUFF & TUFFACEOUS SILTSTONE, LIGHT GREEN, WITH ABUNDANT FRAGMENTS OF LIGHT PINKISH BROWN RHYOLITE LIPS	1000
4000	LOWER & MIDDLE PLEISTOCENE			BASALT, AS ABOVE, WITH TUFF AND SILTSTONE BETWEEN FLOWS	
				SAND, WHITE, VERY FINE TO MEDIUM GRAINED, WELL SORTED, ARGILL - CONTAINS TROUSSEAU AND GILSHUTE IN THE J.H. JAMES NO. 1 WELL	
				SAND, SILTSTONE, TUFF, AND MELDED TUFF, INTERBEDDED	
5000				BASALT, BLACK, PYRITHE & PLAGIOCLASE	1500
6000		Basalts of the Columbia River Group (?) or Banbury Basalts (?)		SAND, VERY FINE TO COARSE GRAINED & SILICA CEMENTED SANDSTONE	
				SAND, WHITE TO LIGHT BROWN, VERY FINE TO FINE GRAINED, POORLY SORTED	
7000				BASALT, ALTERED TO A DARK GREEN, ZEOLITE IN ARGILLULES	2000
8000				SANDSTONE, GRAY-WHITE, ARGILLIC WITH LITHIC FRAGMENTS, VERY FINE TO COARSE GRAINED, MODERATELY SORTED	
		Deer Butte Formation (?)		SILTSTONE, LIGHT TO DARK BROWN, LAMINATED, INTERBEDDED WITH MODERATELY SORTED ARGILLIC SANDSTONE	2500
9000	MIocene			BASALT, BLACK, ZEOLITE IN ARGILLULES	
				MELDED TUFF, VERY COLORFUL, GRAY-BROWN-GREEN, QUARTZ AND PLAGIOCLASE PHENOCRYSTS	
		Owyhee Basalts (?)		BASALT, BLACK TO DARK GREEN INTERBEDDED WITH VITRIC AND LITHIC TUFFS	
				BASALT, BLACK TO DARK GREEN, PASSIVE THICK FLOWS CHALCOPHY AND ZEOLITE IN ARGILLULES	
10000				SANDSTONE, WHITE TO CREAM, FINE TO COARSE GRAINED TUFACEOUS	
				TUFF, LIGHT TO MEDIUM GRAY, MELDED IN PART ASHY IN PART, QUARTZ AND FELDSPAR PHENOCRYSTS, AND ALTERED GLASS - INTERBEDDED GRAY-BROWN CLAY AND BROWN SILTSTONE	3000
11000		Lower Sucker Creek Formation		SANDSTONE, MILKY-WHITE, POORLY SORTED, CLAYEY TUFF, AS ABOVE	
12000				TUFF, DARK GREEN TO GRAY AND LAVENDER, PARTLY HARD VITRIC AND LITHIC TUFF, INTERBEDDED WITH LIGHT AND DARK BROWN SILTSTONE	3500
13000				BASALT, DARK GRAY TO DARK GREEN, ABUNDANT EMBEDDED PLAGIOCLASE (LATHS), SUBORDINATE OLIVINE (?)	
				RHYOLITE-DACITE TUFF, MOTTLED GRAY-LAVENDER, QUARTZ AND OLIVINE (?) PHENOCRYSTS	
		Older Owyhee Rhyolites & welded tuffs		INTERBEDDED VITRIC AND LITHIC TUFFS AND GRAY TO LAVENDER MELDED TUFFS, SPHERULITIC IN PART, PROGRADE, APHILLIC, AND QUARTZ PHENOCRYSTS	4000
				LATHS AND RHYOLITE AND DACITE (?) FLOWS & TUFFS, PHENOCRYSTS OF AMPHIBOLE AND BIOTITE	
14000	MIocene (?)	Older Lathes & Basalts, undivided			

FIGURE 4.—Composite stratigraphic column of Nampa-Caldwell area. This column was produced by correlating data from five wells in or immediately outside study area by S. H. Wood, and is used here with his permission.

where $g(S)$ is the observed gravity in mgals at station S , $g(B)$ is the observed gravity in mgals at a base station B , R_s is the gravimeter reading at station S , and R_B is the gravimeter reading at base station B . All observed gravity values are ultimately referenced to an absolute gravity station (DOD station 1302-0) at Ontario, Oregon. The station is located at the Ontario airport on a concrete sidewalk at ground level against the first step at the westernmost entrance on the north side of the Air West terminal building. It was set in June 1974 by the Department of Defense. The IGSN value of this station is 980,289.78 mgals.

The reduction program then computes a theoretical gravity value for station S as follows:

$$g_{TH}(S) = g(d) + FC + BC \quad (2)$$

where $g_{TH}(S)$ is the theoretical gravity for S , d is the latitude of S , $g(d)$ is the gravity at latitude (d) calculated from the International Gravity Formula (Swick 1942), FC is the free-air correction (-0.09406 mgal per foot of elevation above mean sea level), and BC is the Bouguer correction ($+0.01276 \rho$ mgal per foot of elevation above mean sea level where ρ is the Bouguer slab density in gm/cc). The Bouguer slab density for this study was chosen to be 2.0 gm/cc on the basis of densities obtained from the formation density logs of the James no. 1 and Higgenson no. 1 wells, both located immediately east of the study area.

Finally, the reduction program computes a Bouguer anomaly value for station S :

$$\Delta g(S) = g(S) - g_{TH}(S) \quad (3)$$

The Bouguer anomaly values are output in a listing that includes details of the computation process.

It is important to note that the program makes a drift correction to each R_s of a loop before calculation of $g(S)$. Drift caused by tides and instrument factors is assumed to be linear between end readings of a three- to four-hour loop made from a field base.

Terrain Corrections

Terrain corrections were done through Zone I, maximum radius 14,612 feet (Hammer 1939). Because of the low topographic profile of the area, it was felt that terrain corrections through Zone I would be sufficiently accurate. Altogether 58 stations were terrain corrected. Terrain corrections of less than 0.05 mgals were ignored. The maximum terrain correction was 0.18 mgals. The average terrain correction for those 28 stations with 0.05 mgals correction or more was 0.09 mgals (standard deviation 0.04 mgals).

The terrain-corrected Bouguer gravity anomaly for the Bouguer density of 2.0 gm/cc was hand contoured at a 1 mgal interval (fig. 5).

Reliability of Data

The total error in gravity data represents an accumulation of several small errors.

The gravimeter used in the survey gave repeatable readings within 0.03 mgals. The maximum change due to drift observed during a single loop was 0.42 mgals. The mean drift over a single loop was 0.11 mgals (standard deviation 0.01 mgals). The reduction routine corrected for drift assuming linearity with time, when in reality this variation departs somewhat from true linearity even over a very short time. The amount of error due to drift is reduced when loop times are shortened. The largest loop time was 5.85 hours, the mean loop time was 3.10 hours (standard deviation 0.99 hours).

Instrument reading was plotted against time for all base station #1 readings (fig. 6). It shows a steady increase in readings over the survey period (six weeks), with only low-frequency and low-amplitude departures during that period. This indicates that no "tear" exists in the data due to problems with the gravimeter.

Before the survey began, the instrument calibration was checked by "looping" it twice over a standard course. The instrument checked out to within 0.00 mgals of the standard established by the University of Utah.

Another major source of errors in gravity data is due to imprecise horizontal locations and elevations of gravity stations. Virtually all the stations in the survey are located at road intersections, section or quarter corners, bench marks, or easily recognizable landmarks. The topographic sheets are accurate to 1/50 of an inch which corresponds to about 40 feet on a ground reference. The error in station location probably did not exceed 100 feet in the north-south direction, which would result in a maximum error in theoretical gravity of about 0.025 mgals at this latitude. The locations were digitized with a maximum error of 0.05 minute of an arc. This would result in a theoretical gravity error of 0.055 mgals at this latitude if the mislocation is in a north-south direction. Therefore the maximum total error due to horizontal mislocation is probably about 0.080 mgals.

Ten percent of the stations were at first or second order bench marks, 33 percent were at corners with published elevation, and the remaining 57 percent were interpolated from contour lines taken directly from the topographical sheets. The maximum error would occur in the last category (57%). The contours are accurate to one-half the contour interval. Seventy-seven percent of the area was covered with topographic sheets, which had a 10-foot contour interval and 5-foot intermediates, which would result in a maximum error of from 2.5 feet to 5 feet, or 0.15 to 0.30 mgals in theoretical gravity. Twenty-three percent of the area was covered with topographic sheets having a 20-foot contour interval with 10-foot intermediates, which would result in a maximum error of from 5 to 10 feet or 0.30 to 0.60 mgals in theoretical gravity. Therefore, the total maximum error due to inaccurate elevations is about 0.60 mgals. Hand leveling between landmarks of known elevation probably reduced this error somewhat.

Terrain corrections of less than 0.05 mgals were ignored; therefore, the maximum error in theoretical gravity due to terrain is 0.05 mgals. Eight and five-tenths percent of the stations were terrain corrected. Fifty percent of those corrected had terrain corrections which exceeded 0.05 mgals.

GRAVITY DATA ANALYSIS

Terrain-Corrected Bouguer Gravity Anomaly Map

To facilitate the interpretation of the processed gravity data the terrain-corrected Bouguer gravity anomaly was hand-contoured onto a base map (fig. 5). The datum is mean sea level, the Bouguer density is 2.0 gm/cc, and the contour interval is 1 mgal. It was felt that this contour interval would optimize the visual interpretation of gravity anomalies. A smaller interval would tend to clutter the map, and a larger interval would fail to make efficient use of the gravity data and would undoubtedly obscure some anomalies. The map was originally drawn to a scale of 1:48,000 so as to conform to published topographic base maps, as well as other maps currently in preparation by the Idaho Department of Water Resources, but, like the preliminary geologic map by Spencer H. Wood (fig. 3), is included herein at page size to be used with the gravity data maps. It

is included to show relationships between gravity anomalies and surface geology.

The most striking feature of the terrain-corrected Bouguer anomaly map (fig. 5) is the strong northwest regional trend. This trend is consistent with the regional gravity and the magnetic and structural fabric of the High Lava Plains geomorphic

subprovince. It has been interpreted by Hill (1963), Mabey (1976), and Warner (1975) to be the result of crustal thinning, normal block faulting forming grabenlike structures, and infill with sediments and volcanics. The cause of such activity is believed to be pre-Tertiary rifting and left-lateral movement centering near the course of the present Snake River, followed by

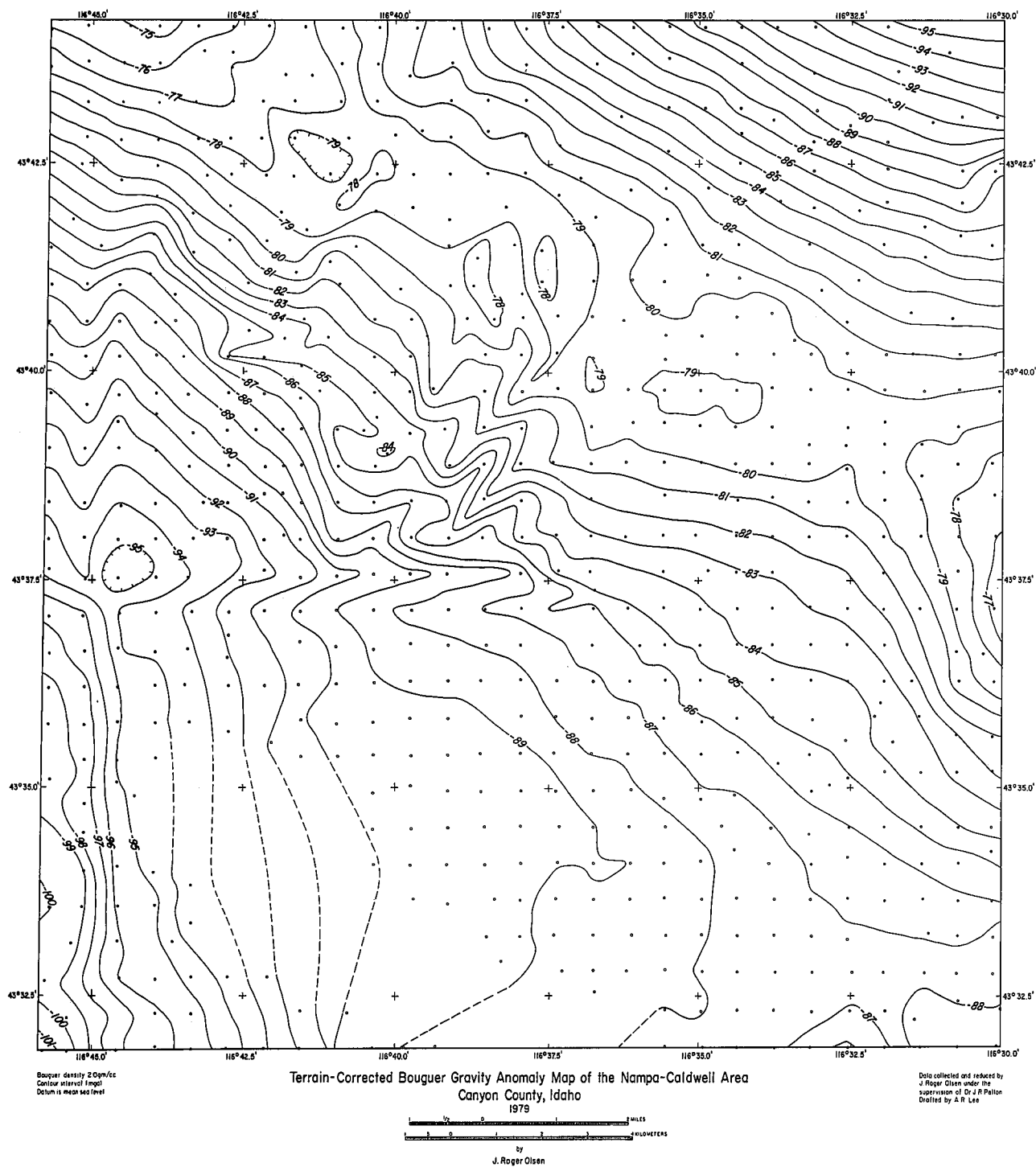


FIGURE 5.—Terrain-corrected Bouguer gravity anomaly map.

Tertiary downwarping and/or faulting (Warner 1975).

Because the regional gravity anomaly is so large and uniform, only generalizations may be made regarding local gravity anomalies.

Near the left center margin of the map there is an area of closure which appears to be due to the intersection of two structural features, one trending to the north and the other to the east. The sinusoidal nature of these anomalies is suggestive of normal faults or long narrow grabens and horsts (Telford and others 1976, p. 19). It is puzzling why these features run contrary to the regional trend and die out so abruptly.

High-frequency anomalies near the center of the map are probably due to near-surface features such as isolated basalt flows, basalt flow surface irregularities, erosional remnants of basalts, and/or minor fault blocks. This map was shown to Spencer H. Wood, who agreed that the more specific interpretations of local, near-surface anomalies are best made on the basis of the residual gravity anomaly.

Third-Order Residual Gravity Anomaly Map

The regional, low-frequency gravity anomaly is assumed to originate from large deep-seated sources whereas high frequency residual anomalies are assumed to arise from near-surface, more localized geologic features. Because a broad shallow source can produce the same anomalies as a deep source, there is some ambiguity arising from the above assumptions. The technique used in this study for separating the regional from the residual gravity anomalies was polynomial fitting. This method assumes that the regional gravity anomaly may be approximated by a low-order polynomial of two independent variables.

Using computer programs developed at the University of Utah, I first calculated a polynomial which would best approximate the regional gravity field. The program, using the complete Bouguer anomaly data from the area, chooses constants which define a polynomial of specified order such that the least square error between the polynomial and the data is minimized.

Constants from the polynomial thus calculated were then put into a residual program with the Bouguer gravity anomaly data to calculate the residual gravity anomaly, or the difference between the original terrain-corrected Bouguer anomaly and an anomaly calculated at that same point using the polynomial.

On the basis of inspection it was felt that a third-order polynomial would best fit the regional gravity anomaly observed on the terrain-corrected Bouguer gravity anomaly map (fig. 5). Higher orders would tend to pick up the local anomalies, while a lower-order polynomial would not adequately remove the regional field.

Both the regional and residual gravity anomalies were hand contoured, the regional at an interval of 1.0 mgals and the residual at an interval of 0.5 mgals.

Regional Gravity Map

The regional gravity map (fig. 7) is included mainly for the purpose of showing the shape of the field removed from the terrain-corrected Bouguer anomaly to yield the residual gravity anomaly. It corresponds quite well to the regional Bouguer gravity map prepared by Mabey and Peterson (1974).

In the southwest quarter of figure 7 a deep gravity low is partially developed. It may have been produced by lack of data near Lake Lowell because the polynomial was not constrained by data in the area, and the fit was made by extrapolation over great distances. Because of the possibility that this low in the polynomial surface may be artificial, the residual high indicated in the Lake Lowell area (fig. 8) may also be an artifact. Nevertheless, the shape of the regional low (fig. 7) is not incompatible with the regional gravity map of Mabey and Peterson (1974), and geologic data tend to support its existence. It will therefore be modeled as if it were real.

INTERPRETATION

Residual Gravity Anomaly Map—General Remarks

Before 2½-dimensional modeling can be meaningfully undertaken, gravity anomalies must be interpreted intuitively in light of all known geologic data. I will here note some observations and suggest possible explanations for the most prominent of the anomalies expressed on the residual gravity anomaly map (fig. 8).

The most striking feature of the map is the triangular gravity low (A to D and 2 to 5, fig. 9). This feature is formed by the intersection of a strong north-south-trending anomaly near the western border of the map and an east-west-trending anomaly near the center of the map. The hypotenuse is formed by a group of strong high-frequency anomalies trending north-westward.

The north-south-trending anomaly may be interpreted as a buried fault. There is no surface expression of this feature, but data from the Richardson No. 1 well (fig. 2) indicate that a fault with a displacement of at least 500 feet has lowered this area relative to the area on the west. Wood (1979) suggests that the faulting occurs at a depth of about 1000 feet on the upthrown side. The trend of this anomaly continues nearly the entire length of the western border of the area though its character changes abruptly between 5 and 6 (fig. 9). The reason for the change is open to many possibilities: (1) the nature of the regional gravity removed in the southwest quarter of the map, as explained earlier; (2) masking of the feature by surface basalts in the Lake Lowell area; (3) greater movement along the fault north of what may be an east-west-trending fault (between 5 and 6, A to D, fig. 9); a north-south scissor fault with a fulcrum near 5.5 (fig. 9). It is puzzling why the anomaly dies

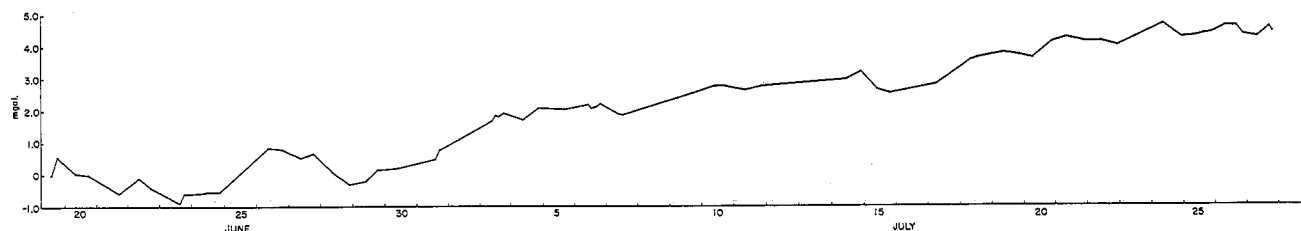


FIGURE 6.—Instrument-performance record for the time the data was collected in the field (June and July 1978) showing general upward trend with only low-frequency and low-amplitude departures from point of beginning, indicating that instrument functioned well during entire survey.

out so abruptly in the north though masking by near-surface basalts may be the answer. This problem will be dealt with in more detail in a later section.

The east-west anomaly forming the base of the triangle may also be a fault at a similar depth and of a similar displacement to the one just described. It dies out abruptly on the east end but appears possibly to continue to the west near the border of the area. As with the southern end of the north-trending anomaly, the character of the feature appears to have

changed on the west. I envision a near-surface basalt flow, trending northwestward, to be masking the south and west ends of these intersecting anomalies. This supposition is substantiated by shallow-well data in the area.

The high-frequency anomaly complex that forms the hypotenuse of this anomaly triangle is possibly the result of near-surface flows. The irregularity is probably the result of a combination of deposition on an irregular surface, flowage around topographically positive areas, dissection by streams, and fault-

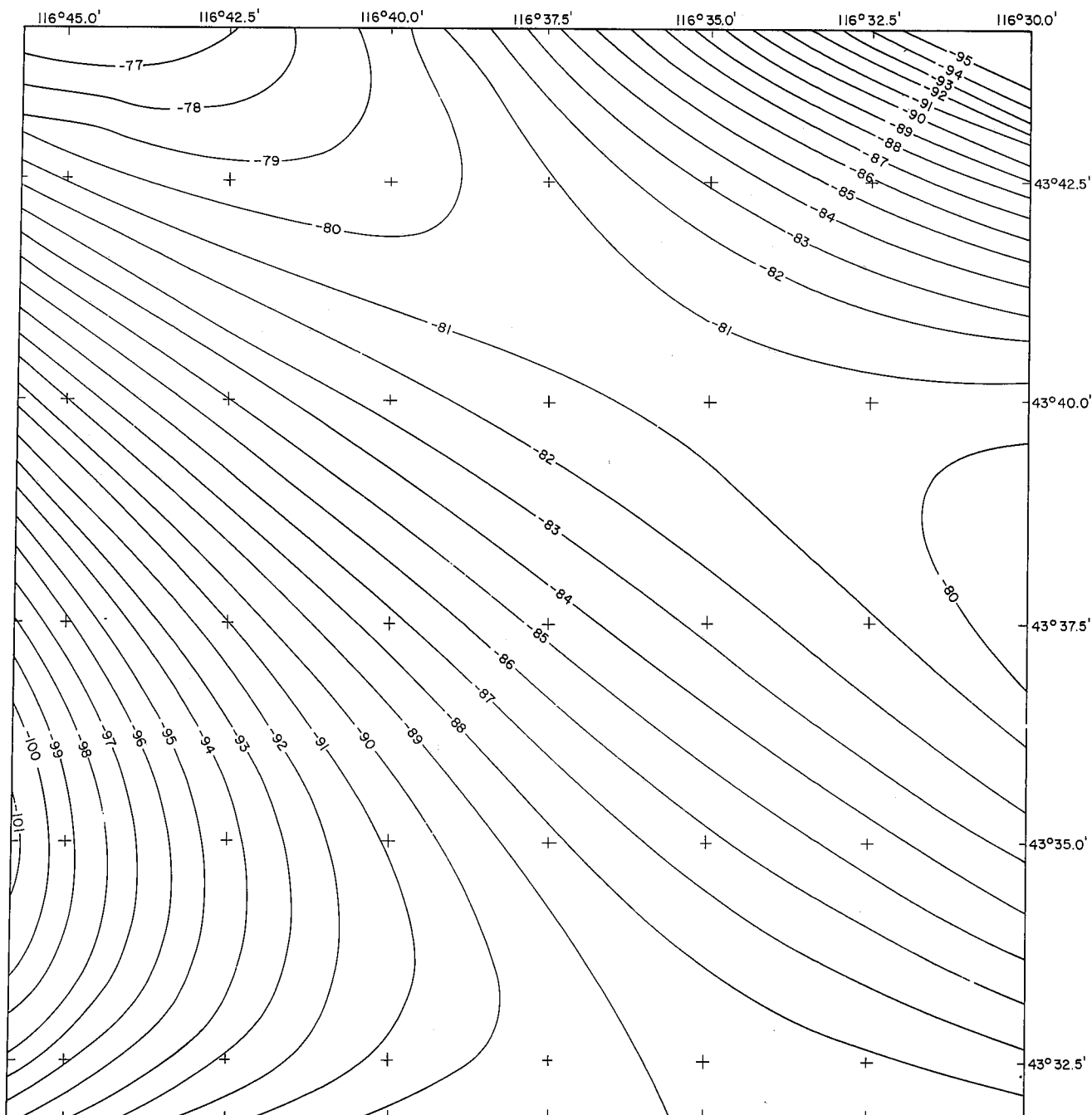


FIGURE 7.—Third-order polynomial model shows shape and magnitude of regional gravity anomaly removed from complete Bouguer anomaly to yield residual gravity anomaly.

ing. Well data in the area attest to structural complexity in the subsurface. It is interesting to note that this complex anomaly parallels the regional gravity high.

In an area where the entire structural fabric trends north-west, it is puzzling why the anomalies forming the arms of the right triangle trend north-south and east-west. Rotation into

the present position seems unlikely on the basis of the inferred geologic history of the area (Warner 1977).

Another explanation is that the anomaly triangle is not formed by faults, but rather that it represents flowage of basalt around a low-density erosional remnant. It seems unlikely (though not impossible) that the anomaly represents a triangular downdropped block.

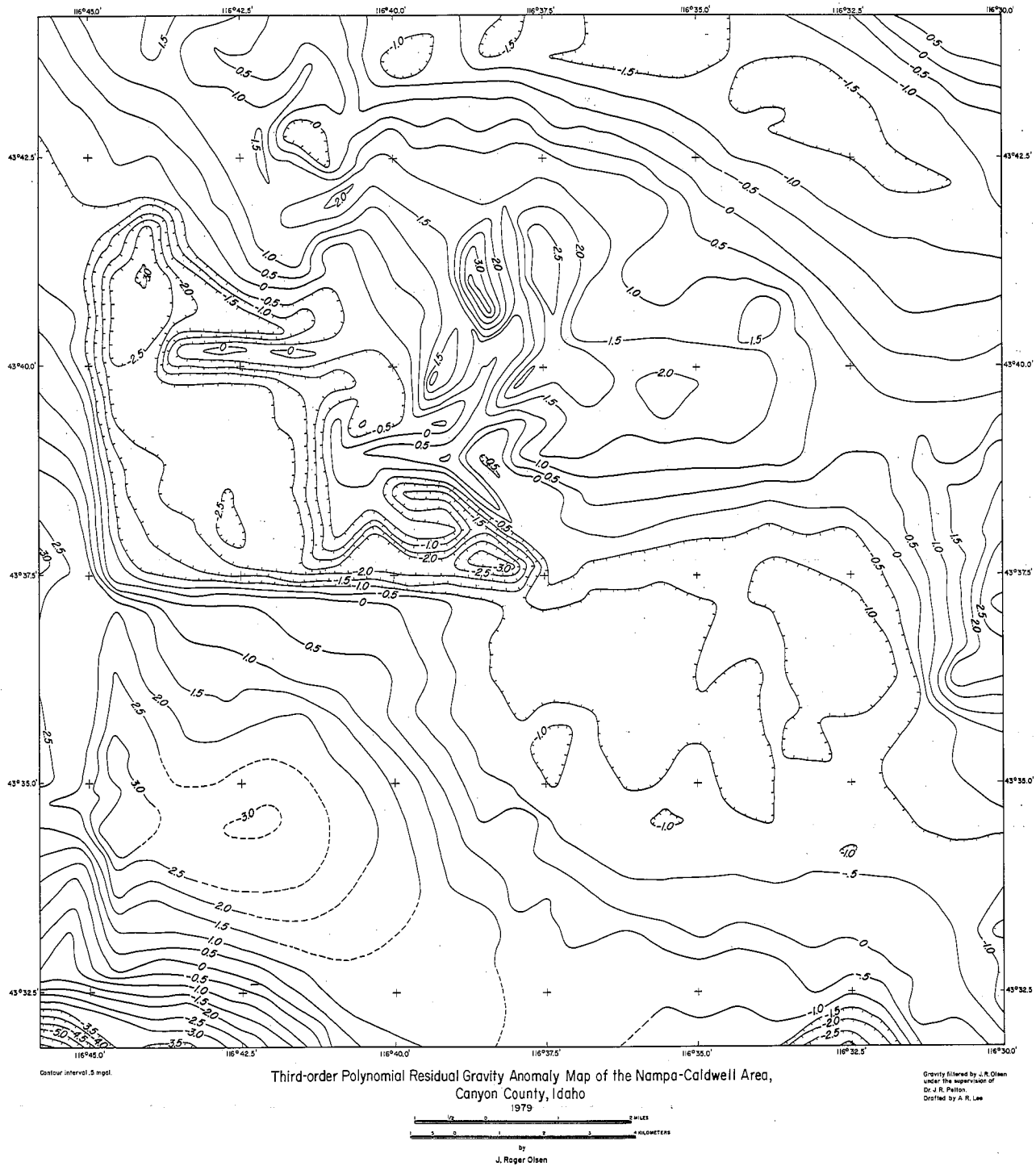


FIGURE 8.—Third-order polynomial residual gravity anomaly map.

I feel that it would be hard to dispute the idea that this anomaly represents the combined effects of faults, basalt flows, and other structural features superimposed on one another.

Another interesting anomaly occurs in the Lake Lowell

area. It consists of a gravity high forming an area of closure over a topographic low. As mentioned earlier, this anomaly may be an artifact formed when the regional gravity was removed. On the basis of shallow drill-hole data and surface map-

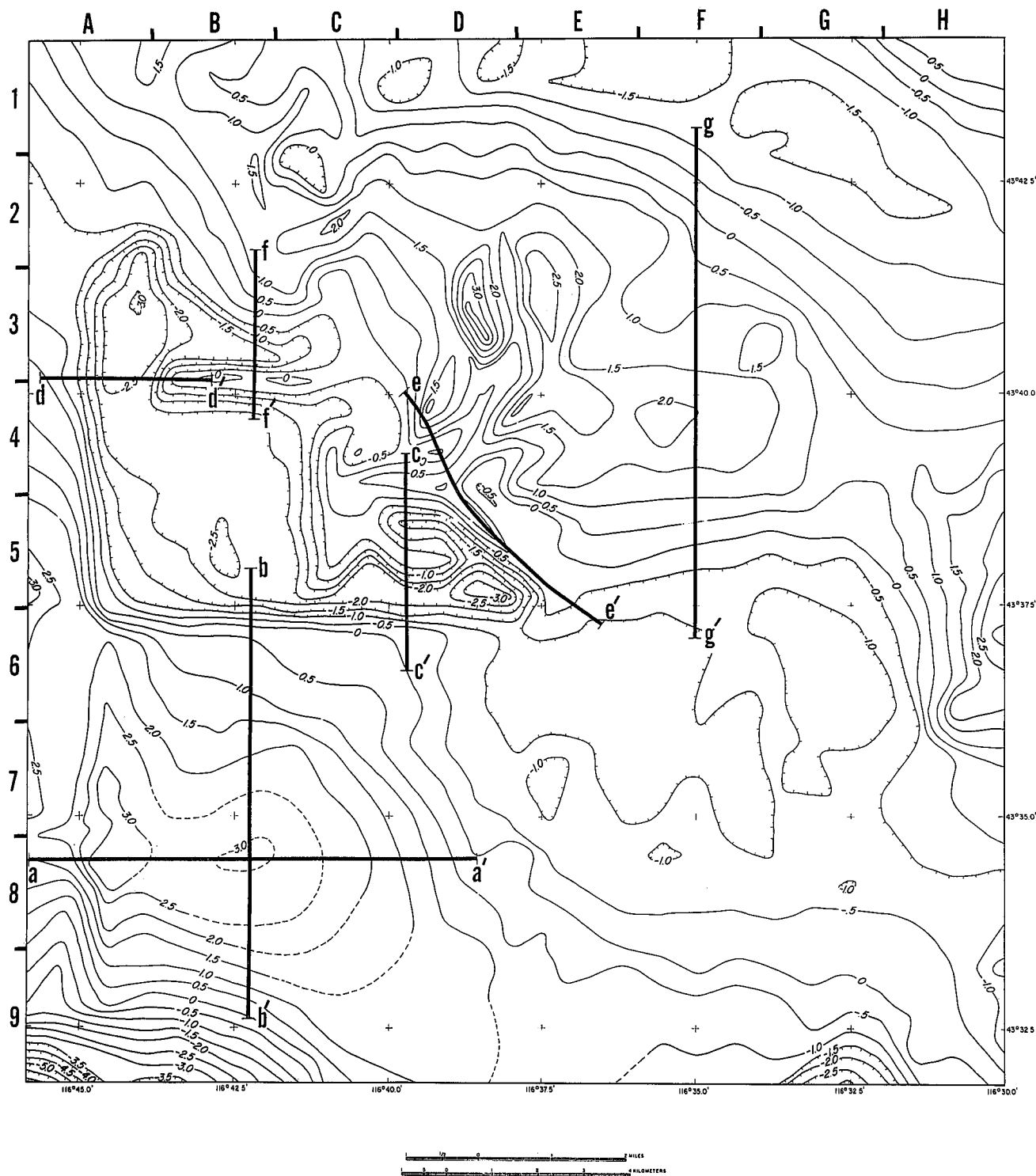


FIGURE 9.—Third-order polynomial residual gravity anomaly map showing locations of gravity profiles. Letters along top and numbers down left side are used for locating anomalies referred to in text.

ping (fig. 3), the area appears to be a graben. The gravity high is possibly formed by a shallow basalt which flowed into the same basin where Lake Lowell is now, though renewed movement along faults and downwarp may have deepened it after the deposition of basalt.

From the northwest corner through the east central border of the area, the northwest grain of the terrain-corrected Bouguer anomaly map still persists. It is quite possible that a northwest-trending fault zone along the southwestern edge of the trough truncated the north and east extensions of the linear features described earlier, burying all traces of them under sequences of volcanics and alluvium.

I have here presented what I believe to be the most plausible interpretations of the observed data in light of what is currently known about the subsurface geology of the Nampa-Caldwell area. Alternate interpretations for these, as well as other smaller or less pronounced anomalies, may be necessary when more information becomes available.

Profile Modeling

Modeling of selected gravity profiles was accomplished with the use of an inversion program developed by J. H. Snow (unpublished) at the University of Utah. In this program the forward gravity problem is computed using a $2\frac{1}{2}$ -dimensional algorithm developed by Cady (1977). Linear inversion adjusts nodal vertices of polygonal cross sections and density contrasts to obtain a better fit of the computed anomalies to the observed anomalies (Carter and others 1978).

Profile locations were chosen in areas where gravity anomalies were most pronounced, and also where at least some geologic control existed or where some geologic interpretations had already been made on the basis of known geology. Altogether five profiles were modeled. The $2\frac{1}{2}$ -dimensional program allows independent specification of positive and negative strike lengths, which were chosen to give the best fit to the anomaly being modeled. Densities were based on borehole formation density logs or were inferred on the basis of known or assumed rock types.

Gravity values were either taken directly from the residual gravity anomaly map (fig. 8) or were measured directly in the field. For the values obtained from the residual gravity anomaly map, the regional gravity was assumed to have been adequately removed. For the detailed gravity profiles measurements were made directly in the field and subsequently reduced to residual values.

The subsurface geology in the study area appears to be very complex on the basis of gravity data as well as other geologic information. The models are accurate only insofar as the assumptions on which they are based are accurate. There are an infinite variety of combinations of geologic parameters which may produce a given gravity anomaly. I have tried to reduce this ambiguity by basing the models on all currently available geologic data for the area.

Gravity Profile a-a' and Interpretative Model.

Gravity values interpolated directly from the third-order polynomial residual map (fig. 8) were used for profile a-a' (fig. 10) along a 32,000-foot east-west line crossing Lake Lowell (see 8A to D, fig. 9). The Lake Lowell area is a topographic low which may be a graben (Wood 1979). The preliminary geologic map (fig. 3) indicates normal faulting on both the northeast and southwest sides of the lake. All the faults in this area strike northward with the down-dropped blocks nearest the lake (Wood pers. comm. 1979). Shallow well data (lithologic logs)

show a "lava" (basalt?) flow encountered to not more than 100 feet below the surface. It ranges in thickness from a few feet to more than 300 feet, and preflow and postflow faulting is evident. In some areas other "lava" and cinder units are encountered at greater depths.

For the sake of this model I assumed a single homogeneous flow with no faulting. The flow was assumed to be basalt with a density of 3.0 gm/cc resting in a basin of unconsolidated clastic sediments of density 2.1 gm/cc, which gives a density contrast of 0.9 gm/cc. The strike lengths used were 8,000 feet in both directions. It was assumed that the flow was flat-topped and exposed at the surface. A "perfect fit" was not sought in modeling this profile because of the lack of gravity and geologic data, but, as can be seen in figure 10, a good general fit was obtained. The total sum of the squares is 6.273, the variance is 0.216, and the standard deviation is 0.465.

The model shows a basalt slab with a flat top and an irregular bottom. It is impossible to show the placement of faults on the basis of so few geologic data. This model is meant to show the general configuration of a surface flow which would produce the given residual gravity anomaly (compare profile b-b' and interpretive model).

Gravity Profile b-b' and Interpretive Model

Gravity profile and interpretive model b-b' (fig. 11) cross the Lake Lowell area perpendicular to profile a-a' (see 5-9B, fig. 9). This profile is also 32,000 feet long. Gravity values were obtained by direct interpolation from the third-order residual gravity anomaly map (fig. 8).

For this model a basalt flow of density 3.0 gm/cm³ was assumed to lie on unconsolidated clastic sediments of density 2.1 gm/cc giving a density contrast of 0.9 gm/cm³. The flow was assumed to be flat topped, but unlike model a-a' is thicker and covered by a 100-foot blanket of sediment. Well data and surface mapping indicate that the flow (in some areas) is buried to about 100 feet. The basalt was assumed to be homogeneous and unfaulted. A strike length of 8,000 feet was used in both directions. As with profile a-a', a perfect fit was not sought in modeling profile b-b'. A reasonably close fit was obtained which gave a total sum of the squares value of 3.259, a variance of 0.105, and a standard deviation of 0.324.

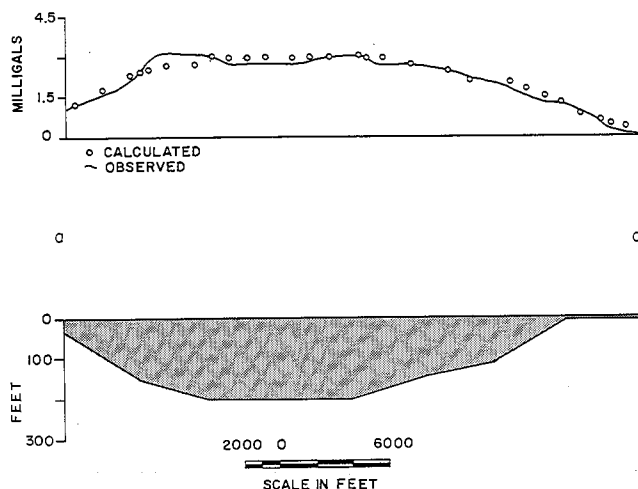


FIGURE 10.—Gravity profile a-a' and $2\frac{1}{2}$ dimensional interpretive model. The density contrast is 0.9 gm/cc and the strike lengths are 8000 feet in both directions.

The deepest part of the flow (where gravity is highest) in both models a-a' and b-b' occurs very near the topographic low point in Lake Lowell. This suggests that downwarping and/or faulting may be in part postflow and makes the assumption doubtful. In both profiles a-a' and b-b' the assumed basalt layer may be in reality thinner or less continuous than as modeled, making the gravity anomaly due, in part, to some other source such as multiple flows. The idea of a buried intrusion seems unlikely to account for the anomaly on the basis of regional and local geology and history (Warner 1977). A high-density erosional remnant is another possibility, but I am skeptical because of known regional and local geology.

Gravity Profile c-c' and Interpretive Model

Profile c-c' was taken along a 15,400-foot north-south line (fig. 12; C/D4-6, fig. 9). Gravity values for the northern mile of this profile were interpolated from the residual gravity anomaly map (fig. 8), and values for the remaining part of the profile were taken from a detailed gravity survey with a station spacing of 500 feet. Elevations for the profile were obtained by running a level line along the profile route.

Shallow-well data indicate a great deal of structural complexity in the area of this profile. Generally speaking, the very near-surface (500 feet or less) basalts in both wells and in surface outcrop are not nearly thick enough to account for the entire anomaly though they no doubt contribute to it.

Because of the lack of subsurface geologic information, it would be futile to try to model exact locations and structures of basalts or other rock bodies in any detail. This model attempts to show the distribution and general configuration of a flow which might be responsible for producing this anomaly. A basalt having a density of 3.0 gm/cc buried below surface sediments of density 2.2 gm/cc is assumed. This gives a density contrast of 0.8 gm/cc. A strike length of 1,000 feet was used in both directions. A good fit was obtained for this model. The total sum of the squares 0.670, the variance is 0.032, and the standard deviation is 0.179.

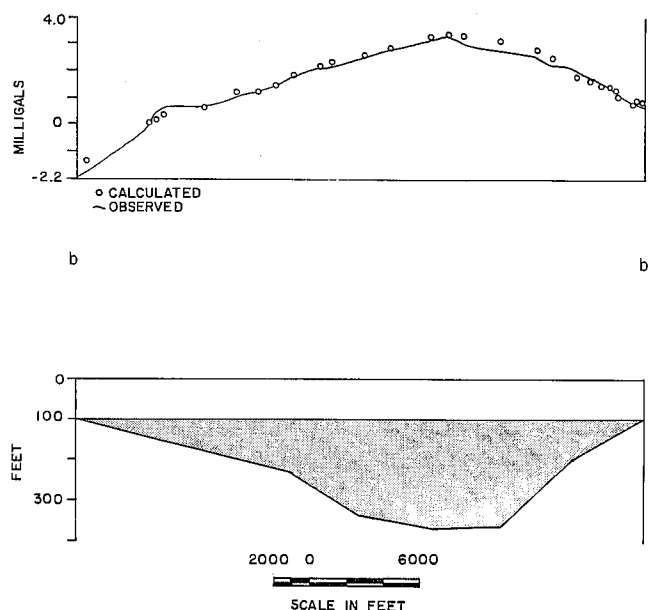


FIGURE 11.—Gravity profile b-b' and 2½ dimensional interpretive model. The density contrast is 0.9 gm/cc and the strike lengths are 8000 feet in both directions.

Gravity Profile d-d' and Interpretive Model

Gravity Profile d-d' is an east-west profile 8,500 feet in length (3/4 A-B, fig. 9). For this profile gravity measurements were taken every 500 feet, and elevations were determined by leveling (fig. 13).

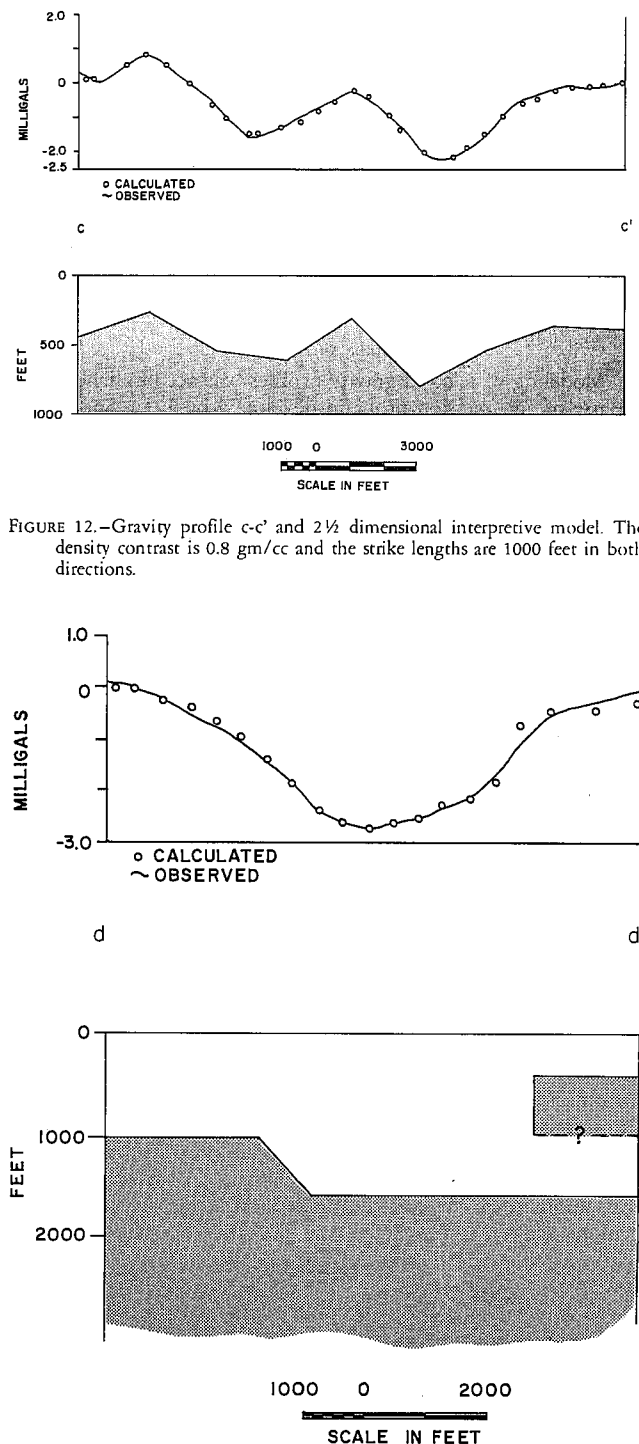


FIGURE 12.—Gravity profile c-c' and 2½ dimensional interpretive model. The density contrast is 0.8 gm/cc and the strike lengths are 1000 feet in both directions.

FIGURE 13.—Gravity profile d-d' and 2½ dimensional interpretive model. The density contrast is 0.8 gm/cc and the strike lengths are 8000 feet in both directions.

For this model the strong north-south-trending anomaly which the profile crosses is assumed to be a fault. Correlation of drill-hole data indicates that a fault (or faults) exists somewhere west of the Richardson No. 1 well (see fig. 2 for location). Well data indicate that the throw of the fault (if a single fault is involved) is at least 500 feet. I made the top of the basalt on the upthrown block in the model to lie at a depth of 1,000 feet as well data indicate that burial is at least that deep. A "slab" of basalt was inserted at the right side of the model to represent the near-surface flow.

A good fit was obtained during the inversion portion of the modeling process. The sum of the squares was 0.481, the variance was 0.034, and the standard deviation was 0.185. It must be understood that, if the fault is actually deeper than as modeled, the throw must be increased. Likewise, if the density contrast is less than 0.8 gm/cc (it is doubtful that it would be greater), the throw would again be increased.

Gravity Profile e-e'

Profile e-e' is a detailed profile taken along Interstate 80N (fig. 9). It is 24,000 feet long. Gravity measurements were made at stations spaced along the profile at 500-foot intervals. Elevations were obtained from interstate highway plans.

No models were made for this profile because of its complexity, variable strike lengths, and lack of geologic control. It is included here only to show its complexity (fig. 14).

Gravity Profile f-f' and Interpretive Model

Gravity profile f-f' is taken along a north-south line 12,000 feet long (fig. 15; B2-3, fig. 9). The gravity values for this profile were interpolated directly from the third-order residual gravity anomaly map. For this reason a "perfect fit" was not sought. A reasonably close fit was obtained, however, which yielded a total sum of the squares of 0.616, a variance of 0.031, and a standard deviation of 0.176.

The flow in the model may have been dissected by streams, faulted, downwarped, or deposited on an uneven surface. The areal shape of the anomaly may also have been controlled by basalt flowing around low-density surface features, such as hills. The sharp right angles in the model are obviously unrealistic for basalt flows.

Gravity Profile g-g' and Interpretive Models

Gravity profile g-g' was taken along a north-south line 36,000 feet long, (F1 to 6, fig. 9). Gravity values for the profile were taken directly from the residual gravity anomaly map (fig. 8).

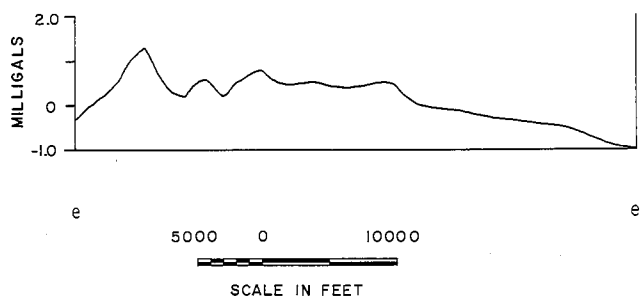


FIGURE 14.—Gravity profile e-e'. No interpretive model was done for this profile.

Because of lack of deep-well data in the immediate area of the profile, the depths and thicknesses of flows are not known. For this reason three models were made to show the configuration of a sequence of flows of variable thickness and depth which would produce the observed anomaly. The first model (fig. 16) had a total sum of the squares of 1.170, a variance of 0.051, and a standard deviation of 0.226. The second model (fig. 17) yielded a total sum of the squares of 1.792, a variance of 0.075, and a standard deviation of 0.273. The third model (fig. 18) yielded a total sum of squares of 1.790, a variance of 0.081, and a standard deviation of 0.285.

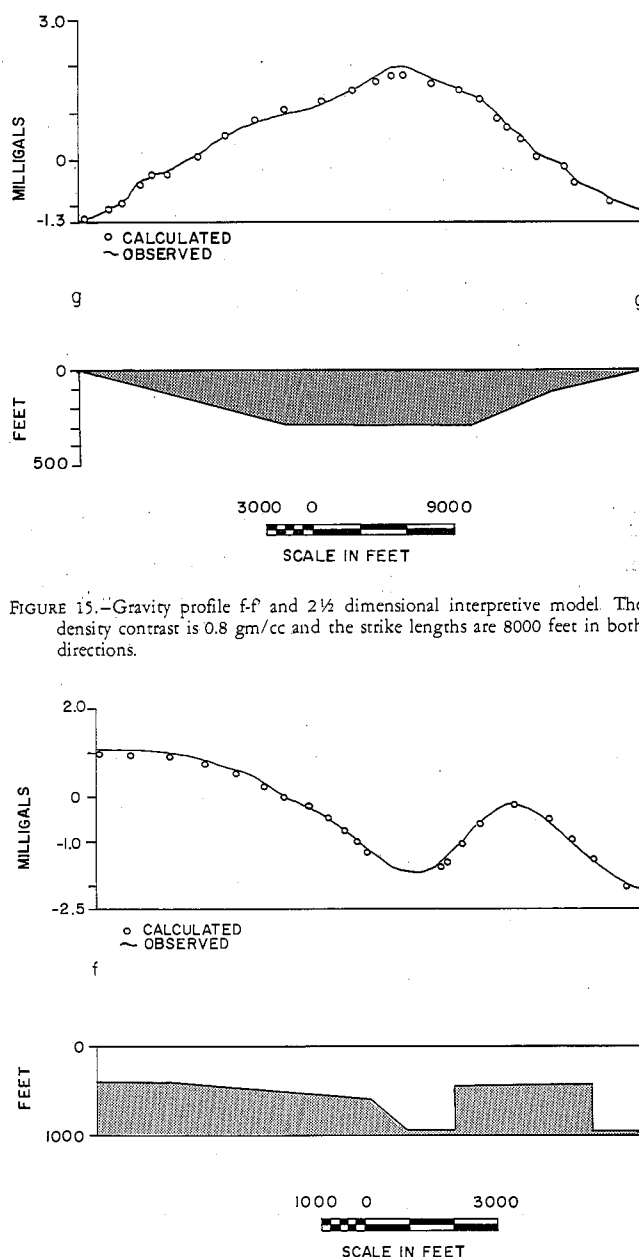


FIGURE 15.—Gravity profile f-f' and 2 1/2 dimensional interpretive model. The density contrast is 0.8 gm/cc and the strike lengths are 8000 feet in both directions.

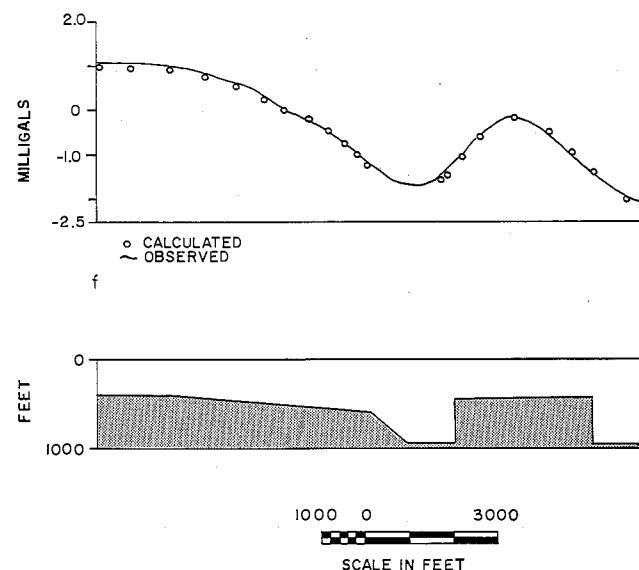


FIGURE 16.—Gravity profile g-g' and 2 1/2 dimensional interpretive model. The density contrast is 0.8 gm/cc and the strike lengths are 6000 feet.

SUMMARY AND CONCLUSIONS

The gravity study of the Nampa-Caldwell area in Canyon County in western Idaho is part of an integrated geological and geophysical study being done by the Idaho Department of Water Resources Geothermal Division to better evaluate the geothermal potential of the area. Gravity was measured at 680 stations in an area of 182 square miles with an average station spacing of .05 miles. The data were reduced by computer using a program which first calculated theoretical gravity using the international gravity formula, then applied a free air correction of -0.09406 mgal per foot of elevation above mean sea level and a Bouguer correction of $+0.01276 \rho$ mgal per foot of elevation above mean sea level, where ρ is the Bouguer slab density in g/cc. The simple Bouguer anomaly was hand terrain-corrected using the method of Hammer (1939). Linear drift corrections were made at the time of data reduction by the reduction program.

The terrain-corrected Bouguer anomaly map of the Nampa-Caldwell area indicates three types of anomalies: (1) a strong (15–20 mgal) northwest-trending regional high, (2) linear anomalies trending north-south and east-west, and (3) anomalies of high spatial frequency with complex orientation. To emphasize the local anomalies and depress the regional gravity high, a third-order polynomial was fitted to the terrain-corrected Bouguer anomaly map and removed from the data.

Features of the third-order polynomial residual gravity map are: (1) a strong (5 mgal) right-triangular-shaped anomaly in the northwest part of the area; (2) high-frequency anomalies which form the hypotenuse of the triangular anomaly, and (3) a closed anomaly in the Lake Lowell area. The "arms" of the right-triangular anomaly have been interpreted as faults. The same anomaly could also be produced by a buried low-density erosional remnant. The high-frequency anomalies probably represent complexities in subsurface basalts. The anomaly over Lake Lowell may result from a near-surface basalt flow in a structural basin but may also be an artifact of map processing. The residual gravity anomaly map has inherited the northwest-trending fabric of the Bouguer anomaly map. Faulting and downwarp along a northwest trend may have truncated the "arms" of the triangular anomaly, obscuring them under volcanics and sediments. Masking by near-surface basalts may be obscuring traces of this anomaly in the south and west.

Two and one-half-dimensional interpretive modeling was done over selected anomalies. The purpose of all the models was to suggest possible geologic features which could produce the observed anomalies. Density contrasts were based on formation density logs or were inferred from lithologic data. The models give a good general idea of the possible configurations of anomaly-producing structures, but no definite conclusions are implied because of lack of geologic control.

The appendix to this paper, manuscript pages 58–80, is on open file in the Geology Department, Brigham Young University, Provo, Utah 84602, where a Xerox copy may be obtained.

REFERENCES CITED

- Armstrong, R. L., Leeman, W. P., and Malde, H. E., 1975, K-Ar dating Quaternary and Neogene volcanic rocks of the Snake River Plain, Idaho: *American Journal of Science* v. 275, p. 225–51.
- Birkeland, P. W., Crandell, D. R., and Richmond, G. M., 1971, Status of correlation of Quaternary stratigraphic units of the western continental United States: *Quaternary Research*, v. 1, p. 208–27.
- Buwalda, J. P., 1923, A preliminary reconnaissance of the gas and oil possibilities of southwestern and south central Idaho: Idaho Bureau of Mines and Geology Pamphlets 5, p. 3.

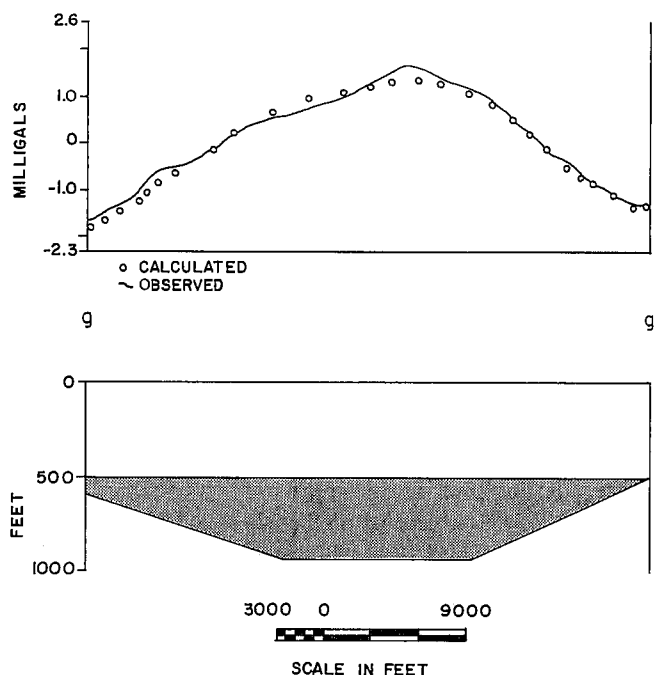


FIGURE 17.—Gravity profile $g-g'$ and 2½ dimensional interpretive model showing alternative interpretation of the observed anomaly. The density contrast is 0.8 gm/cc and the strike lengths are 6000 feet.

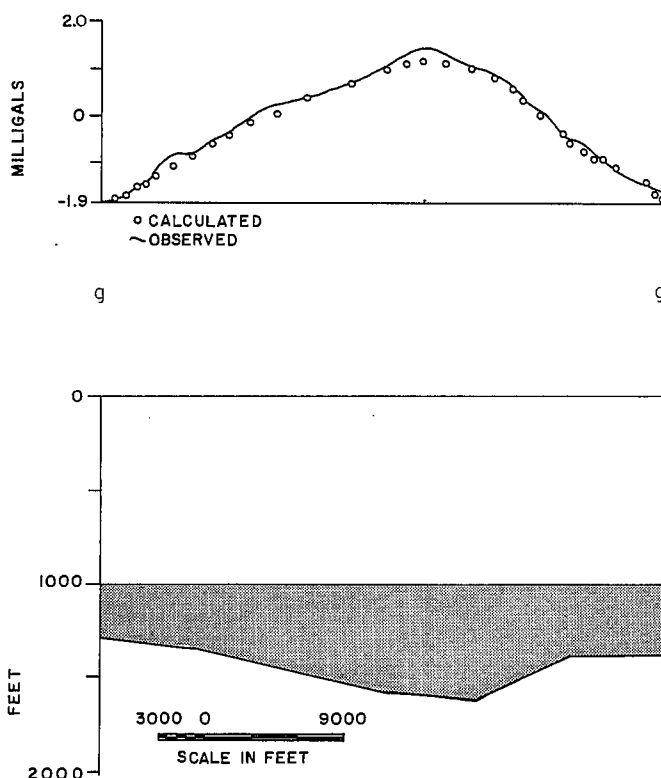


FIGURE 18.—Gravity profile $g-g'$ and 2½ dimensional interpretive model showing alternative interpretation of the observed anomaly. The density contrast is 0.8 gm/cc and the strike lengths are 6000 feet.

- Carter, J. A., and Cook, K. L., 1978, Regional gravity and aeromagnetic surveys of the Mineral Mountains and vicinity, Millard and Beaver Counties, Utah: Master's thesis, University of Utah, Salt Lake City.
- Cady, J. W., 1977, Calculation of gravity and magnetic anomalies along profiles with end corrections and inverse solutions for density and magnetization: U.S. Geological Survey Open File Report, no. 77-463, 110p.
- Dobrin, M. B., 1976, Introduction to geophysical prospecting, 3rd ed.: McGraw-Hill, New York.
- Ekren, E. B., McIntyre, D. H., and Bennett, E. H., 1978, Preliminary geologic map of the west half of Owyhee County, Idaho: U.S. Geological Survey Open File Report 78-341. 1:125,000.
- Evernden, J. F., Savage, D. E., Curtis, G. H., and James, G. T., 1964, Potassium-argon dates and the Cenozoic mammalian chronology of North America: American Journal of Science, v. 262, p. 145-98.
- Freeman, O. W., Forrester, J. D., and Luper, R. L., 1945, Physiographic divisions of the Columbia intermontane province: Association of American Geographers Annals, v. 35, p. 53-75.
- Hammer, S., 1939, Terrain corrections for gravimeter stations: Geophysics, v. 4, p. 184-94.
- Hill, D. P., 1963, Gravity and crustal structure in the western Snake River Plain, Idaho: Journal of Geophysical Research, v. 68, p. 5807-18.
- Hill, D. P., 1972, Crustal and upper mantle structure of the Columbia Plateau from long range seismic refraction measurements: Geological Society of America Bulletin, v. 83, p. 1639-48.
- Hill, D. P., and Pakiser, L. C., 1965, Crustal structure between the Nevada test site and Boise, Idaho, from seismic-refraction measurements, in the earth beneath the continents: American Geophysics Union, Geophysics Monthly, v. 10, p. 391-419.
- Kirkham, V. R. D., 1931a, Revision of the Payette and Idaho Formations: Journal of Geology, v. 39, p. 193-239.
- , 1931b, Snake River downwarp: Journal of Geology, v. 39, no. 5, p. 456-82.
- , 1931c, Igneous geology of southwestern Idaho: Journal of Geology, v. 39, no. 6, p. 564-91.
- Kittleman, L. R., Green, A. R., Hagood, A. R., Johnson, A. M., McMurray, J. M., Russell, R. G., and Weeden, D. A., 1965, Cenozoic stratigraphy of the Owyhee region, southeastern Oregon: Bulletin 1, Museum of Natural History, University of Oregon—Eugene, 45p.
- Lindgren, W., 1898, Description of the Boise Quadrangle, Geologic Atlas of the United States: U.S. Geological Survey, folio 45. 1:125,000.
- Lindgren, W., and Dranke, N. F., 1904, Description of the Nampa Quadrangle, Idaho, Oregon, Geologic Atlas of the United States: U.S. Geological Survey, folio 103.
- Mabey, D. R., 1976, Interpretation of a gravity profile across the western Snake River Plain, Idaho: Geology, v. 4, p. 53 1/2.
- Mabey, D. R., Peterson, D. L., and Wilson, C. W., 1974, Preliminary gravity map of southern Idaho: U.S. Geological Survey Open File Report.
- Malde, H. E., 1965, Snake River Plain, in the Quaternary of the United States: Princeton, N. J.: Princeton University Press, p. 255-63.
- Malde, H. E., and Powers, H. A., 1962, Upper Cenozoic stratigraphy of western Snake River Plain, Idaho, Geological Society of America Bulletin, v. 73, p. 1197-1220.
- Malde, H. E., Powers, H. A., and Marshall, C. H., 1963, Reconnaissance geologic map of west-central Snake River Plain, Idaho: U.S. Geological Survey Miscellaneous Geology Investigation Map I-373. 1:125,000.
- Manger, G. E., 1966, Handbook of physical constants, rev. ed.: Geological Society of America Memoir 97.
- Nace, R. L., West, S. W., and Mower, R. W., 1957, Feasibility of groundwater features of the alternate plan for the Mountain Home project, Idaho: U.S. Geological Survey Water-Supply Paper 1376, 121p.
- Newton, V. C., and Corcoran, R. E., 1963, Petroleum geology of the western Snake River Basin, Oregon-Idaho: Oregon Department of Geology and Mineral Industries. Oil and Gas Investigations, no. 1, 67p.
- Priest, T. W., Case, C. W., Wittry, J. E., Preece, R. K., Jr., Monroe, G. A., Biggerstaff, H. W., Logan, G. H., Rasmussen, L. M., and Webb, D. H., 1972, Soil survey of Canyon County area, Idaho: U.S. Department of Agriculture, Soil Conservation Service, 118p. 1:20,000.
- Savage, C. N., 1958, Geology and mineral resources of Ada and Canyon counties, Idaho: Idaho Bureau of Mines and Geology County Report 3, 94p. 1:125,000.
- Swick, C. H., 1942, Pendulum gravity measurements and isostatic reductions: U.S. Coast and Geologic Special Publication 232.
- Telford, W. M., Geldart, L. P., Sheriff, R. E., and Keys, D. A., 1976, Applied geophysics: Cambridge University Press, Cambridge, United Kingdom.
- Taubeneck, W. H., 1971, Idaho batholith and its southern extension: Geologic Society of America Bulletin v. 82, p. 1899-1928.
- Thornbury, W. D., 1965, Regional geomorphology of the United States: John Wiley and Sons, New York, p. 461-62.
- Warner, M. M., 1975, Special aspects of Cenozoic history of southern Idaho and their geothermal implications: In Proceedings, 13th Annual Engineering Geology and Soils Engineering Symposium, p. 247-70.
- , 1977, The Cenozoic of the Snake River Plain of Idaho: 29th Annual Field Conference, 1977 Wyoming Geological Association Guidebook, p. 313-26.
- Wood, S. H., 1979, Surface and subsurface area geology of the Nampa-Caldwell area: Unpublished manuscript, Boise State University, Boise, Idaho.
- , 1979, Preliminary geologic map of Nampa-Caldwell area, Boise State University, Boise, Idaho.

